



**HAL**  
open science

## **ALCAM (CD166) is involved in extravasation of monocytes rather than T cells across the blood–brain barrier**

Ruth Lyck, Marc-André Lécuyer, Michael Abadier, Christof Wyss, Christoph Matti, Maria Rosito, Gaby Enzmann, Thomas Zeis, Laure Michel, Ana García Martín, et al.

### ► To cite this version:

Ruth Lyck, Marc-André Lécuyer, Michael Abadier, Christof Wyss, Christoph Matti, et al.. ALCAM (CD166) is involved in extravasation of monocytes rather than T cells across the blood–brain barrier. *Journal of Cerebral Blood Flow and Metabolism*, 2017, 37 (8), pp.2894-2909. 10.1177/0271678X16678639 . hal-02506628

**HAL Id: hal-02506628**

**<https://univ-artois.hal.science/hal-02506628v1>**

Submitted on 10 Jan 2022

**HAL** is a multi-disciplinary open access archive for the deposit and dissemination of scientific research documents, whether they are published or not. The documents may come from teaching and research institutions in France or abroad, or from public or private research centers.

L'archive ouverte pluridisciplinaire **HAL**, est destinée au dépôt et à la diffusion de documents scientifiques de niveau recherche, publiés ou non, émanant des établissements d'enseignement et de recherche français ou étrangers, des laboratoires publics ou privés.



Distributed under a Creative Commons Attribution - NonCommercial 4.0 International License



**HAL**  
open science

## **ALCAM (CD166) is involved in extravasation of monocytes rather than T cells across the blood–brain barrier**

Ruth Lyck, Marc-André Lécuyer, Michael Abadier, Christof Wyss, Christoph Matti, Maria Rosito, Gaby Enzmann, Thomas Zeis, Laure Michel, Ana García Martín, et al.

### ► To cite this version:

Ruth Lyck, Marc-André Lécuyer, Michael Abadier, Christof Wyss, Christoph Matti, et al.. ALCAM (CD166) is involved in extravasation of monocytes rather than T cells across the blood–brain barrier. *Journal of Cerebral Blood Flow and Metabolism*, Nature Publishing Group, 2017, 37 (8), pp.2894-2909. 10.1177/0271678X16678639 . hal-02506628

**HAL Id: hal-02506628**

**<https://hal-univ-artois.archives-ouvertes.fr/hal-02506628>**

Submitted on 10 Jan 2022

**HAL** is a multi-disciplinary open access archive for the deposit and dissemination of scientific research documents, whether they are published or not. The documents may come from teaching and research institutions in France or abroad, or from public or private research centers.

L'archive ouverte pluridisciplinaire **HAL**, est destinée au dépôt et à la diffusion de documents scientifiques de niveau recherche, publiés ou non, émanant des établissements d'enseignement et de recherche français ou étrangers, des laboratoires publics ou privés.



Distributed under a Creative Commons Attribution-NonCommercial 4.0 International License

---

# ALCAM (CD166) is involved in extravasation of monocytes rather than T cells across the blood–brain barrier

Ruth Lyck<sup>1,\*</sup>, Marc-André Lécuyer<sup>2,\*</sup>, Michael Abadier<sup>1</sup>, Christof B Wyss<sup>1</sup>, Christoph Matti<sup>1</sup>, Maria Rosito<sup>1</sup>, Gaby Enzmann<sup>1</sup>, Thomas Zeis<sup>3</sup>, Laure Michel<sup>2</sup>, Ana B García Martín<sup>1</sup>, Federica Sallusto<sup>4</sup>, Fabien Gosselet<sup>5</sup>, Urban Deutsch<sup>1</sup>, Joshua A Weiner<sup>6</sup>, Nicole Schaeren-Wiemers<sup>3</sup>, Alexandre Prat<sup>2,\*</sup> and Britta Engelhardt<sup>1,\*</sup>

## Abstract

Activated leukocyte cell adhesion molecule (ALCAM) has been proposed to mediate leukocyte migration across the blood–brain barrier (BBB) in multiple sclerosis or experimental autoimmune encephalomyelitis (EAE). Here, we confirmed vascular ALCAM expression in human brain tissue samples *in situ* and on two different human *in vitro* BBB models. Antibody-mediated inhibition of ALCAM reduced diapedesis of human CD4<sup>+</sup> Th1 but not of Th17 cells across the human BBB *in vitro*. In accordance to human Th1 cells, mouse Th1 cells showed reduced diapedesis across an ALCAM<sup>-/-</sup> *in vitro* BBB model under static but no longer under flow conditions. In contrast to the limited role of ALCAM in T cell extravasation across the BBB, we found a contribution of ALCAM to rolling, adhesion, and diapedesis of human CD14<sup>+</sup> monocytes across the human BBB under flow and static conditions. Taken together, our study highlights the potential differences in the CNS expression of ALCAM in mouse and human and supports a prominent role for ALCAM in the multi-step extravasation of monocytes across the BBB.

## Keywords

ALCAM, blood–brain barrier, immune cell extravasation, multiple sclerosis, neuroinflammation

Received 9 August 2016; Revised 5 October 2016; Accepted 11 October 2016

## Introduction

The blood–brain barrier (BBB) is formed by microvascular endothelial cells (ECs) of the central nervous system (CNS). It establishes a particularly tight endothelial barrier that protects the brain and spinal cord parenchyma from the changeable milieu in the blood stream while also limiting immune cell trafficking into the CNS.<sup>1</sup> During autoimmune neuroinflammation such as multiple sclerosis (MS) or its animal model, experimental autoimmune encephalomyelitis (EAE), high numbers of immune cells extravasate across the BBB and critically contribute to disease pathogenesis.<sup>2</sup> Preventing immune cell entry into the CNS has been successfully translated into the clinic with the release of the humanized anti- $\alpha$ 4-integrin antibody natalizumab.<sup>3</sup>

---

<sup>1</sup>Theodor Kocher Institute, University of Bern, Bern, Switzerland

<sup>2</sup>Centre de Recherche du Centre Hospitalier de l'Université de Montréal (CRCHUM), Neuroimmunology Research Laboratory, Montréal, Québec, Canada

<sup>3</sup>Neurobiology, Department of Biomedicine, University Hospital Basel, University of Basel, Basel, Switzerland

<sup>4</sup>Institute for Research in Biomedicine, Bellinzona, Switzerland

<sup>5</sup>Sciences Faculty Jean Perrin, Artois University, France

<sup>6</sup>Departments of Biology and Psychiatry, The University of Iowa, Iowa City, IA, USA

\*These authors contributed equally to this work.

## Corresponding author:

Ruth Lyck, Theodor Kocher Institute, University of Bern, Freiestrasse 1, P.O. Box 938, CH-3000, Bern 9.  
Email: ruth.lyck@tki.unibe.ch

However, the low but serious concurrent risk of progressive multifocal leukoencephalopathy (PML) makes pressing the need for more detailed knowledge on the extravasation of autoaggressive immune cells across the BBB.

Extravasation of immune cells across the BBB is a highly dynamic multi-step process mediated by the sequential interaction of cell adhesion and signaling molecules on the immune cell surface with their respective endothelial counter receptors.<sup>4</sup> In vivo and in vitro live cell imaging have revealed that upon firm adhesion, effector T cells not only resist flow, but polarize and crawl along the luminal face of the BBB endothelium until they reach a site permissive for transcellular or paracellular diapedesis.<sup>5–10</sup> In this way, EC adhesion molecules and their leukocyte ligands fulfill critical roles. Previously, we have shown an essential role for intercellular adhesion molecule (ICAM)-1 and vascular cell adhesion molecule (VCAM)-1 in shear resistant arrest of encephalitogenic CD4<sup>+</sup> Th1 cells. We have also demonstrated that high level of ICAM-1 is involved during CD4<sup>+</sup> Th1 cell crawling against the flow and favors a transcellular diapedesis across the BBB.<sup>5,6</sup>

Activated leukocyte cell adhesion molecule (ALCAM; CD166) on human and mouse brain ECs has also been assigned a role in the extravasation of CD4<sup>+</sup> T cells across the BBB and in the development of EAE.<sup>11</sup> Similar to ICAM-1, ALCAM harbors five extracellular immunoglobulin (Ig)-like domains, a single spanning transmembrane domain, and a short cytoplasmic tail.<sup>12–14</sup> During homophilic ALCAM-ALCAM interactions, the first N-terminal Ig-domain of cis-clustered ALCAM binds to the N-terminal Ig-domain of another ALCAM in trans.<sup>15</sup> The stronger heterophilic ALCAM-CD6 interaction is mediated by the N-terminal Ig-domain of ALCAM and the membrane proximal scavenger receptor cysteine-rich (SRCR) domain of CD6.<sup>16</sup> CD6-mediated interaction of T cells<sup>17,18</sup> with ALCAM on antigen presenting cells<sup>19</sup> or on thymic epithelium<sup>12</sup> has been assigned a role in T cell activation and selection of thymocytes, respectively. In humans, the risk for MS development is associated with a distinct ALCAM polymorphism<sup>20</sup> and one MS risk allele, named rs17824933G, is located in intron 1 of the CD6 gene.<sup>21,22</sup> Thus, ALCAM as a BBB specific ligand for neuroinflammatory cells could be an interesting candidate in the search for alternative pharmaceutical targets aiming to prevent pathological immune cell infiltration into the CNS.

We here addressed the role of endothelial ALCAM in the extravasation of immune cell subsets critically involved in EAE and MS pathogenesis across the human and mouse BBB. We revealed differences in the expression of ALCAM on the human versus mouse BBB and delineated a limited role of ALCAM

in the diapedesis of CD4<sup>+</sup> Th1 or Th17 cells across the human or mouse BBB. In contrast, prominent impairment occurred at various steps of CD14<sup>+</sup> monocyte extravasation upon functional blockade of ALCAM. This suggests that ALCAM might influence MS pathogenesis by interfering with myeloid cell recruitment to the CNS but less so with T cells.

## Materials and methods

### Mice

Wild type C57BL/6J mice were obtained from Harlan (Horst, Netherlands) and Janvier (Genest Saint Isle, France). ALCAM<sup>-/-</sup> mice<sup>23</sup> backcrossed into C57BL/6J background for eight or more generations were kindly provided by Prof. Cornelia Halin, ETH Zürich, Switzerland. Mice were housed in individually ventilated cages under specific pathogen-free conditions. Animal procedures were performed in accordance with the Swiss legislation on the protection of animals or the guidelines of the Canadian Council on Animal Care and were approved by the Veterinary Office of the Kanton of Bern or the Centre de Recherche du Centre Hospitalier de l'Université de Montréal (CRCHUM) Animal Care committee (N11023APs).

### In vitro models of the BBB

**Human brain-like endothelial cells.** CD34<sup>+</sup> cells and pericytes were isolated and differentiated exactly as described before.<sup>24,25</sup> For the collection of human umbilical cord blood, infants' parents signed an informed consent form, in compliance with the French legislation. The protocol was approved by the French Ministry of Higher Education and Research (CODE-COH Number DC2011-1321).

**Human brain endothelial cells.** Human brain endothelial cells (HBECs) were isolated from non-epileptic surgical human CNS material (resection path) exactly as published.<sup>11,26,27</sup>

**Human meningeal endothelial cells.** Human meningeal endothelial cells (HMECs) were isolated from leptomeningeal tissue removed from the CNS material. The tissue was extensively washed in PBS, cut into small pieces, and centrifuged at 1045 g for 15 min. The pellet was incubated in collagenase IV (1 mg/ml) (Sigma) at 37°C for 15 min, then washed in culture media and centrifuged at 485 g for 10 min. The pellet was resuspended in culture media and passed through a 30- $\mu$ m nylon filter (Miltenyi). The fraction <30  $\mu$ m was cultured in six-well plates pre-coated with 0.5% gelatin.

**HBECs and HMECs.** Informed consent and ethic approval were given prior to surgery (Centre de Recherche du Centre Hospitalier de l'Université de Montréal research ethic committee approval number HD04.046).

**Primary mouse brain microvascular endothelial cells (pMBMECs).** Isolation and culture of pMBMECs were performed exactly as described before.<sup>5,28</sup> Cytokine stimulation of pMBMECs was done with TNF- $\alpha$  at 10 ng/ml, IL-1 $\beta$  at 20 ng/ml or TNF- $\alpha$ /IFN- $\gamma$  at 10 ng/ml and 100 U/ml for 16–20 h prior to the experiments.

### **Mouse brain or spinal cord microvessels**

Isolation of mouse brain or spinal cord microvessels was performed as described before<sup>29</sup> and immediately processed for protein lysate.

### **Immune cell subsets**

**Ex vivo human CD4<sup>+</sup>CD45RO<sup>+</sup> T cells.** Venous blood samples were obtained from consenting healthy donors in accordance with institutional guidelines (Centre de Recherche du Centre Hospitalier de l'Université de Montréal research ethic committee approval number SL05.022, SL05.023 and BH07.001), and immune cells were isolated as previously published.<sup>30</sup>

**In vitro polarized Th1 or Th17 cells.** Ex vivo human CD4<sup>+</sup>CD45RO<sup>+</sup> T cells were in vitro polarized as previously published.<sup>31</sup> Briefly,  $0.5 \times 10^6$  CD4<sup>+</sup>CD45RO<sup>+</sup> T cells/ml were cultured with autologous monocytes at a 1 to 0.6 ratio and soluble anti-CD3 (clone OKT3 at 2.5  $\mu$ g/ml, eBioscience). For Th17 differentiation recombinant human IL-23 (25 ng/ml), anti-human IL-4 antibody (5  $\mu$ g/ml) and anti-human IFN- $\gamma$  antibody (5  $\mu$ g/ml) were added, whereas IL-12 (10 ng/ml) in the presence of anti-IL-4 was added for Th1 differentiation (all reagents from R&D Systems). Th1 cells were harvested at day 5 and Th17 cells at day 6 of culture to be used in adhesion and transmigration experiments using HMECs or HBECs.

**CD4<sup>+</sup>CD45RO<sup>+</sup> Th1 cells sorted from peripheral blood.** Human CD4<sup>+</sup> CD45RO<sup>+</sup> Th1 cells were directly sorted from healthy human blood donors according to differential expression of chemokine receptors (CXCR3<sup>+</sup>, CCR4<sup>-</sup>, CCR6<sup>-</sup>) as previously described.<sup>32,33</sup> Th1 cells were cultured in the presence of IL-2 (500 U/ml) for a total of 20 days and then employed for adhesion assay.

**Human monocytes.** Ex vivo human CD14<sup>+</sup> monocytes were isolated from venous blood of consenting healthy donors in accordance with institutional guidelines

(Centre de Recherche du Centre Hospitalier de l'Université de Montréal research ethic committee approval number SL05.022, SL05.023 and BH07.001) as previously published.<sup>30</sup> In brief, peripheral blood mononuclear cells were obtained using density gradient centrifugation on Ficoll-Paque<sup>TM</sup> (GE Healthcare) followed by immune-positive MACS<sup>®</sup> beads (Miltenyi) isolation and used directly (ex vivo) for monocyte/endothelial interaction under flow, adhesion, and transmigration experiments with HBECs or HMECs.

**Mouse CD4<sup>+</sup> Th1 cells.** The encephalitogenic CD4<sup>+</sup> proteolipid protein (PLP)<sub>aa139–153</sub> specific Th1 cell line SJL.PLP7 (IFN- $\gamma$ <sup>+</sup>GM-CSF<sup>+</sup>IL-4<sup>-</sup>IL-17<sup>-</sup>) was used for studying mouse Th1 cell interaction with pMBMECs. Activation with the cognate antigen and culture of Th1 cells was as previously published.<sup>5,34</sup>

### **Antibodies and cytokines**

Antibodies and cytokines are named in the figure legends and specified in supplementary material.

### **Immunohistochemistry and ALCAM quantification on human brain tissue**

Human brain tissues were obtained from post-mortem autopsies supplied by the UK Multiple Sclerosis Tissue Bank (UK Multicentre Research Ethics Committee, MREC/02/2/39), funded by the Multiple Sclerosis Society of Great Britain and Northern Ireland (registered charity 207495, Supplementary Table 1). Immunohistochemistry on cryostat sections (12  $\mu$ m) from fresh frozen tissue blocks was performed as described before.<sup>35</sup> ALCAM immunostaining was evaluated by calculating the average signal intensity of all microvessels ( $\varnothing < 15 \mu$ m) in randomly taken pictures from control (30 pictures from 6 cases) and MS cases (NAWM: 28 pictures from 6 cases, chronic Lesion: 21 pictures from 5 cases). Average signal intensities were first calculated for single cases and tissue type and were then compared in between the different tissue types. Differences between the tissue groups were calculated using the student's *t*-test.

### **Immunofluorescence**

**IF staining on human brain-like endothelial cells.** The human in vitro BBB was stimulated as indicated with TNF- $\alpha$  (10 ng/ml), IL-1 $\beta$  (20 ng/ml), or TNF- $\alpha$ /IFN- $\gamma$  (10 ng/ml each) for 16 h and then incubated with mouse anti-human ALCAM antibody clone 105,901 (10  $\mu$ g/ml) or with mouse IgG1 isotype control for 30 min at 37°C. The BBB was washed, fixed in 1% PFA, unspecific binding sites were blocked in skimmed milk (5% in

PBS) and incubated for 45 min with donkey anti mouse IgG-Cy3 (1:500). Images were acquired with a Nikon Eclipse E600 microscope equipped with a digital camera.

**IF staining on HBECs or HMECs.** HBECs or HMECs were grown to confluency in Ibidi  $\mu$ -slides VI<sup>0.4</sup> and then treated for 24 h with TNF- $\alpha$ /IFN- $\gamma$  (at 100 U/ml each). Cells were washed with PBS and then fixed at room temperature with 70% ethanol. Staining was performed as previously reported<sup>36</sup> using anti-human ALCAM antibody clone 105,901 followed by donkey anti-mouse Cy3. TOPRO-3 Iodide (1:300 in Mowiol mounting medium) was used to stain nuclei. Images were acquired with a LEICA SP5 confocal microscope.

### Quantitative RT-PCR

RNA extraction, cDNA synthesis and SYBR green qPCR were done exactly as described before.<sup>6</sup> Primers (Eurogentec S.A., Seraing, Belgium) were as follows. ALCAM (NM\_009655): CTCAGTGTGGGGAATGG (sense) and TTATGCCTTCAGGCTGTCCT (reverse); ICAM-1 (NM\_010493): CACGCTACCTCTGCTCCTG (sense) and TCTGGGATGGATG GATACCT (reverse); and ribosomal protein S16 (Rps16) (the endogenous control) (NM\_013647): GATATTCGGGTCCGTGTGA (sense) and TTGAGATGGACTGTCGGATG (reverse).

### EAE, protein lysates, Western Blot, and protein quantification

Active EAE, Western Blot, and protein quantification were performed according to standard methods. Details are described in supplementary material.

### Adhesion assay

**Adhesion of ex vivo sorted human CD4<sup>+</sup> Th1 cells to human brain-like endothelial cells.** After six days of co-culture with pericytes on 3  $\mu$ m pore size Transwell<sup>®</sup> inserts, human brain-like endothelial cells (HBLECs) were treated with cytokine for 16 h. Both, the HBLECs and human CD4<sup>+</sup> Th1 cells were pre-incubated with mouse anti-human ALCAM antibody (10  $\mu$ g/ml), anti-human ICAM-1 (15  $\mu$ g/ml), or mouse IgG<sub>1</sub> control antibody (15  $\mu$ g/ml) for 30 min at RT. Soon after incubation, 10<sup>4</sup> human Th1 cells labeled with CMFDA cell tracker (Life Technologies, ThermoFisher) were added on top of the human in vitro BBB and allowed to adhere for 30 min. Non-adherent cells were then gently washed away with PBS and cells were fixed with 1% PFA in PBS, blocked in 5% skimmed milk

in PBS and incubated for 45 min with donkey anti mouse Cy3 antibody (1:500). The human in vitro BBB treated with mouse isotype control was incubated after fixation with mouse anti-human VE-cadherin (1:200). Assays were analyzed by fluorescence microscopy (Nikon Eclipse E600) and Th1 bound cells per pre-defined field were determined by counting five fields per filter. Assays were performed in triplicates for each value.

### Diapedesis assay

**Diapedesis of human immune cell subsets across HBECs or HMECs.** HBECs or HMECs (3.5  $\times$  10<sup>4</sup> cells per filter) were grown on gelatin-coated 3  $\mu$ m pore size Boyden chambers (Fisher Scientific) in culture media supplemented with 40% astrocyte-conditioned media for 72 h (to confluency). Where indicated, antibodies specific for ALCAM (clone 105,901, R&D Systems, 30  $\mu$ g/ml), ICAM-1 (clone BBA3, R&D Systems, 10  $\mu$ g/ml) or the appropriate isotype control were added to ECs and immune cell subsets 1 h prior to the experiment. In presence of the blocking or control antibody, a suspension of 1  $\times$  10<sup>6</sup> leukocytes was added to the upper chamber and allowed to migrate for 16–18 h. The absolute number of cells that transmigrated to the lower chamber was then assessed. All conditions were performed in triplicate for each donor.

**Diapedesis of mouse Th1 cells across pMBMECs.** T cell diapedesis across pMBMECs under static conditions was assessed as described before.<sup>5,37</sup>

### Imaging of extravasation under flow

**In vitro live cell imaging of mouse CD4<sup>+</sup> Th1 cell interaction with pMBMEC.** Imaging of mouse Th1 cell dynamic interaction with pMBMECs cultured on matrigel-coated cell culture surfaces ( $\mu$ -dish<sup>35mm-low</sup>, ibidi Vitaris, Baar, Switzerland) was performed as described before.<sup>5,38</sup>

**In vitro live cell imaging of human monocyte, Th1 cell, or Th17 cell interaction with HBECs.** Imaging of human leukocyte subset interaction with HBECs under flow was performed as previously published.<sup>30,39</sup>

### Statistics

Statistical analysis was performed using GraphPad Prism 6.0 software (Graphpad software, La Jolla, CA, USA). Asterisks indicate significant differences (\* $P$  < 0.05, \*\* $P$  < 0.01, \*\*\* $P$  < 0.001 and \*\*\*\* $P$  < 0.0001). Nonspecific differences are without label. Unless otherwise specified, data are expressed

---

as mean  $\pm$  standard error of the mean (SEM) and statistical differences of two groups were calculated by unpaired Student's *t*-test with equal SD.

## Results

### *ALCAM expression in chronic MS lesions in situ and on the human BBB in vitro*

Previously, we have described prominent ALCAM staining on brain vessels in acute MS lesions.<sup>11</sup> Here, we addressed expression of ALCAM in chronic MS lesions. Immunostaining of post-mortem brain tissue from MS cases confirmed ALCAM on small human brain vessels in chronic MS lesions as well as on microvessels in normal appearing white matter (NAWM) and control brain tissue samples (Figure 1(a)). Quantification of staining signal intensity revealed no significant difference of microvascular ALCAM between all three types of human brain samples (Figure 1(b)). ALCAM immunostaining was also detected on large diameter brain vessels, which were, however, excluded from analysis because they are not involved in immune cell extravasation. Thus, unlike in acute MS lesions,<sup>11</sup> microvessels in chronic MS lesions do not show increased ALCAM staining.

In line with our previous observations, we here confirmed ALCAM immunostaining on primary human brain endothelial cells (HBECs) (Figure 1(c)).<sup>11</sup> We further demonstrated ALCAM immunostaining on a second in vitro model of the human BBB established from CD34<sup>+</sup> cell-derived HBLECs (Figure 1(e)).<sup>24,25</sup> Immunofluorescence (IF) staining confirmed upregulation of endothelial ALCAM following stimulation with TNF- $\alpha$ , IL-1 $\beta$ , or a combination of TNF- $\alpha$  and IFN- $\gamma$  (TNF- $\alpha$ /IFN- $\gamma$ ) on HBECs or HBLECs (Figure 1(c) and (e)). Confocal z-stack images over the low height of less than 1  $\mu$ m of HBECs and HBLECs did not allow a clear allocation of ALCAM to the basal or apical face of the brain ECs (Supplementary Figure 1, Supplementary Movies 1 and 2, and data not shown). As leptomeningeal immune cell infiltration is an important aspect in EAE and potentially in MS, we have additionally compared primary cultures of HBECs with primary cultures of HMECs (Figure 1(c)). As opposed to HBECs, HMECs stained more prominently for ALCAM in resting conditions and no significant increase in staining was observed under inflammatory conditions (Figure 1(c)). Differential cell surface expression of ALCAM by HBECs and HMECs was confirmed by flow cytometry analysis, which also confirmed upregulation of ICAM-1 and VCAM-1 on both HBECs and HMECs upon cytokine stimulation (Figure 1(d)).

### *Limited involvement of ALCAM in the interaction of human CD4<sup>+</sup> T cells with the BBB in vitro*

We have previously assigned a role for ALCAM in the extravasation of monocytes and CD4<sup>+</sup> T cells across the human BBB.<sup>11</sup> However, neither the precise effector T cell subset nor the precise step of extravasation affected by blocking ALCAM has been identified. Here, we aimed to address the role of ALCAM in the extravasation of activated CD4<sup>+</sup> Th1 and Th17 cells across the human BBB. First, we tested the adhesion of ex vivo human CD4<sup>+</sup>CD45RO<sup>+</sup> Th1 cells sorted from human peripheral blood as described before.<sup>40</sup> These T cells expressed CD6 and ALCAM on their surface as determined by flow cytometry (Supplementary Figure 2) and readily adhered to HBLECs in a static environment (Figure 2(a) and (b)). As expected, increased numbers of Th1 cells adhered to the cytokine stimulated HBLECs when compared to unstimulated HBLECs (Figure 2(a) and (b)). However, masking ALCAM with a function-blocking antibody did not interfere with Th1 cell adhesion to the unstimulated or stimulated HBLECs. At the same time, antibody-mediated blocking of endothelial ICAM-1 significantly reduced T cell adhesion to the unstimulated and cytokine stimulated HBLECs (Figure 2(a) and (b)). Using an in vitro flow system, we also tested rolling and initial arrest of human in vitro polarized Th1 and Th17 cells on HBECs. Th1 and Th17 cells used for this experiment were generated by in vitro polarization of ex vivo human CD4<sup>+</sup>CD45RO<sup>+</sup> T cells as described.<sup>31</sup> These T cells expressed similar cell surface levels of CD6 but lower cell surface levels of ALCAM when compared to ex vivo sorted Th1 cells (Supplementary Figure 2). The addition of function-blocking anti-ALCAM antibodies to HBECs and Th1 or Th17 cells did neither reduce their rolling nor their arrest on resting or stimulated HBECs (Figure 2(c) and (d) and data not shown). Taken together, we concluded that ALCAM is not involved in rolling, shear resistant arrest, and firm adhesion of human Th1 and Th17 cells to human in vitro models of the BBB.

To address the role of endothelial ALCAM in T cell diapedesis across HBECs, we used a modified Boyden chamber assay. In line with our previous observations, we found that inhibition of ALCAM reduced the diapedesis of ex vivo sorted CD4<sup>+</sup>CD45RO<sup>+</sup> T cells across HBECs (Figure 2(e)).<sup>11</sup> However, no effect of ALCAM blockade occurred when CD4<sup>+</sup>CD45RO<sup>+</sup> T cells were allowed for diapedesis across HMECs (Figure 2(e)). For refinement, we then analyzed the diapedesis of in vitro polarized Th1 versus Th17 cells and observed that pre-treatment of HBECs with the function-blocking anti-ALCAM antibody or pre-treatment

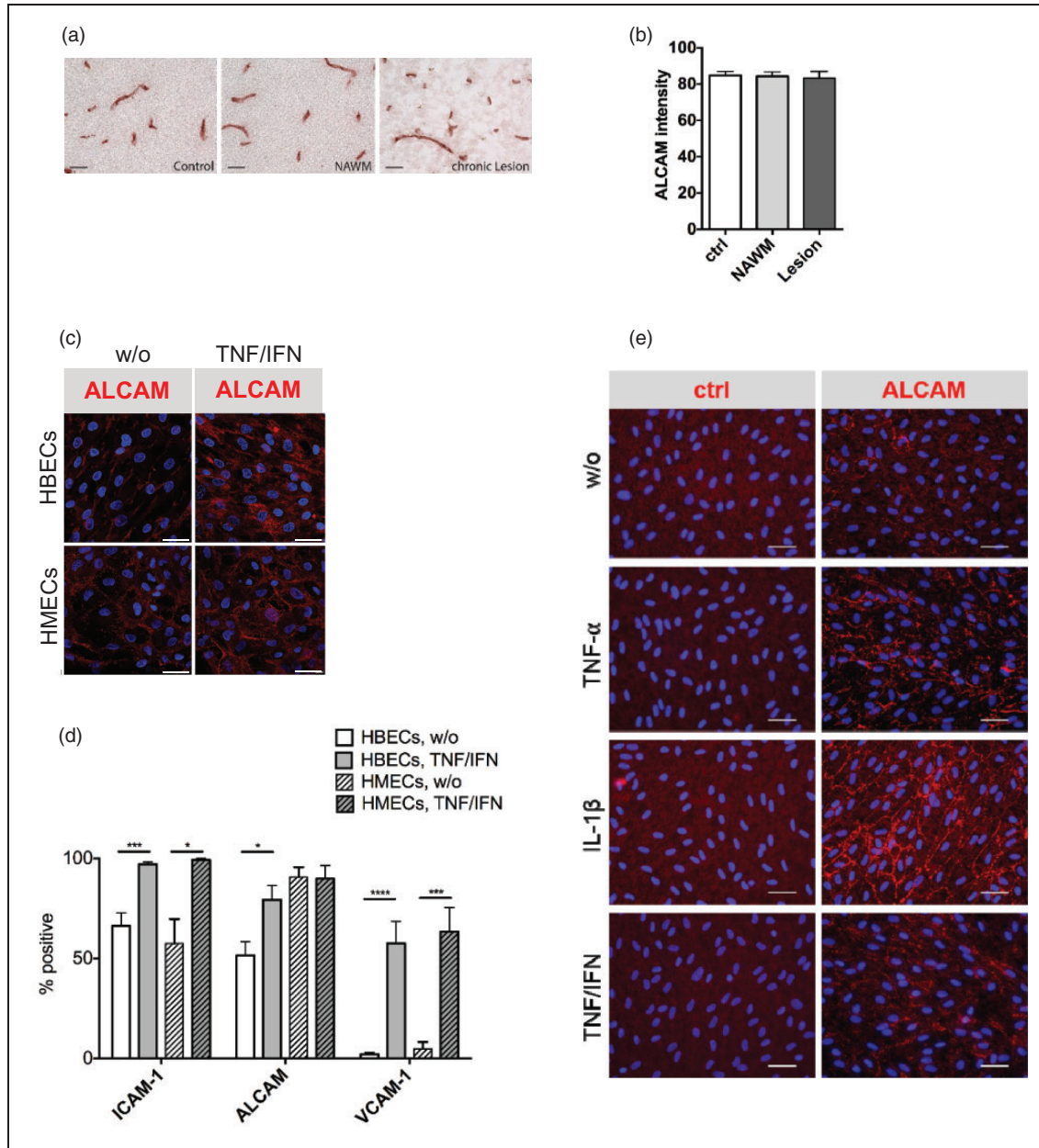


**Figure 1.** ALCAM protein expression on the human BBB. (a) ALCAM expression pattern on control, MS NAWM, and chronic MS lesion tissue samples from the subcortical white matter region of post-mortem human brains as detected by immune histochemistry (polyclonal goat anti-human/mouse ALCAM antibody). Scale bar = 50  $\mu$ m. (b) Densitometry of ALCAM signal intensities on human brain microvessels ( $\varnothing < 15 \mu$ m) as shown in representative images in (a). Randomly taken pictures from control (30 pictures from six cases) and MS cases (NAWM: 28 pictures from six cases, chronic Lesion: 21 pictures from five cases) were evaluated. ALCAM intensity is presented as arbitrary units. (c, e) Anti-ALCAM immunoreactivity (clone 105,901) on unstimulated or cytokine stimulated HBECs and HMECs (c) and HBLECs (e, ctrl, control antibody) is in red. Cytokine stimulation as labeled, nuclei were stained with DAPI (blue). Representative of  $n = 3$  independent experiments. Images were acquired with a 40  $\times$  objective scale bar = 20  $\mu$ m. (d) Quantification of ALCAM (antibody clone 3A6), ICAM-1 (antibody clone HA58), and VCAM-1 (antibody clone 51-10C9) protein expression on HBECs ( $n = 10$ ) or HMECs ( $n = 7$ ) as determined by flow cytometry. Values show % of positive endothelial cells.

of T cells with a function-blocking anti-CD6 antibody significantly reduced diapedesis of Th1 but not of Th17 cells (Figure 2(f) and (g) and data not shown). At the same time antibody-mediated blocking of ICAM-1 had a more pronounced effect on the diapedesis of both T

helper cell subsets across HBECs (Figure 2(f) and (g)). Taken together, blocking ALCAM failed to reduce diapedesis of human  $CD4^+$  Th17 cells across HBECs and exerted a limited effect on the diapedesis of human  $CD4^+$  Th1 cells across the human BBB.

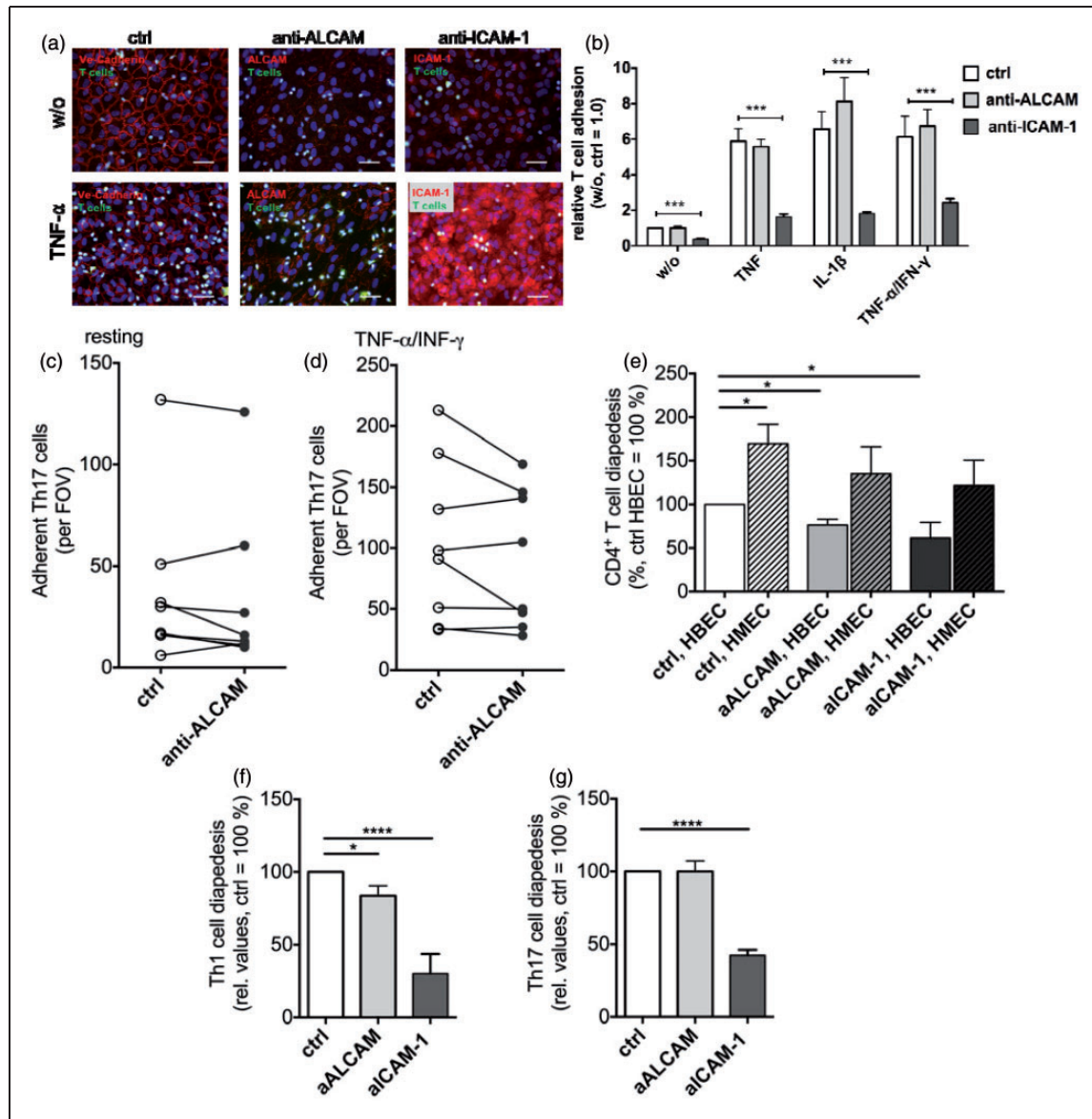


**Figure 2.** Role of ALCAM during the interaction of human Th1 or Th17 cells with HBLECs, HBECs, or HMECs. (a–b) Adhesion of ex vivo sorted human CD4<sup>+</sup> Th1 cells to HBLECs after treatment with function blocking antibodies to ALCAM or ICAM-1 or with isotype control. HBLECs were unstimulated or stimulated with TNF-α (10 ng/ml), IL-1β (20 ng/ml), or TNF-α/IFN-γ (10 ng, 100 U/ml). (a) Representative images of CD4<sup>+</sup> Th1 cells (green, CMFDA loaded) adherent on HBLECs stained for VE-cadherin, ALCAM, or ICAM-1 (red). Cell nuclei are stained with DAPI (blue). Images were acquired with a 40 × objective. Scale bar, 20 μm. (b) Quantification of CD4<sup>+</sup> Th1 cell adhesion to HBLECs. Values are of three independent experiments performed in triplicates and expressed relative to Th1 cell adhesion to isotype control treated, unstimulated HBLECs (1.0). (c–d) numbers of adherent in vitro polarized CD4<sup>+</sup> Th17 cells on resting (c) or cytokine (TNF-α/IFN-γ) stimulated HBLECs 20 min after Th17 cell perfusion. Th17 cells from individual healthy donors are compared side-by-side (Horizontal lines) (n = 8 experiments). (e) Diapedesis of ex vivo human CD4<sup>+</sup>CD45RO<sup>+</sup> T cells across HBECs or HMECs that were pre-treated with ALCAM or ICAM-1 blocking antibodies or isotype control antibody (n = 4). HBECs and HMECs from the same donors were tested side-by-side and diapedesis rates were normalized to T cell diapedesis across isotype control treated HBECs (100%). (f–g), Diapedesis of human in vitro polarized CD4<sup>+</sup> Th1 cells (f) or Th17 cells (g) across unstimulated HBECs that were pre-treated with ALCAM or ICAM-1 blocking antibodies or isotype control antibody (n = 4 experiments). Data are expressed relative to isotype control-treated HBECs (100%). Antibodies were anti ALCAM clone 105,901 (a–g), anti ICAM-1 clone 15.2 (a, b) and clone BBA3 (e–g).

### Prominent neuronal ALCAM masks endothelial ALCAM at the BBB in mice

Research using mouse *in vivo* EAE models or mouse *in vitro* BBB models has been fundamental in improving our understanding of the immune pathogenesis of MS.<sup>41</sup> Previously, we have demonstrated that anti-ALCAM antibody treatment ameliorates MOG<sub>(aa35-55)</sub>-induced EAE in C57BL/6 mice.<sup>11</sup> To determine *in vivo* ALCAM expression in the mouse CNS during EAE, we next analyzed protein lysates from inflamed CNS tissue of C57BL/6 mice suffering from acute EAE compared to age and gender matched healthy controls. The amount of ALCAM protein in lysates from brain cortices and cerebella of EAE mice was comparable to the healthy controls (Figure 3(a) to (c), Supplementary Table 2, Supplementary Figure 3). In contrast, ALCAM levels in spinal cords were lower in EAE, concomitant with an increase of ICAM-1 protein levels, as compared to control samples (Figure 3(a), (d), (e), Supplementary Table 2, Supplementary Figure 3). The presence of two ALCAM bands in the Western Blots of cerebellum and spinal cord lysates presumably represents different post-translational modifications in different CNS cells (Figure 3(a), Supplementary Figure 3). As expected, protein lysates from healthy ALCAM<sup>-/-</sup> C57BL/6 mice were devoid of both ALCAM isoforms (Figure 3(f), Supplementary Figure 3). To localize the cellular sources of ALCAM in the mouse brain, we performed IF staining on frozen naïve brain or spinal cord sections and on respective tissue sections from ALCAM<sup>-/-</sup> mice (Supplementary Figure 4). We found strong ALCAM immunostaining in the meninges of the mouse brain and a more moderate, widespread staining in the parenchyma of the cerebral cortex and the striatum (Supplementary Figure 4(a) and (c)). Strong ALCAM immunoreactivity was also observed in neurons and axons of the dorsal root ganglia, the dorsal, and the ventral horn (Supplementary Figure 4(d) to (f)), and in the axons that projected to a particular dorsal lamina (Supplementary Figure 4(h)). However, multi-color IF staining failed to locate ALCAM staining on IB4-positive CNS vessels in brain and spinal cord sections of C57BL/6 mice (Supplementary Figure 4(j)). We therefore hypothesized that the strong signal intensity of neuronal ALCAM did not allow the detection of lower endothelial ALCAM levels *in situ*.

Therefore, we next tested the expression of ALCAM on freshly isolated CNS vessels and in primary mouse brain microvascular ECs (pMBMECs) from C57BL/6 mice. ALCAM protein was readily detectable in protein lysates from brain and spinal cord vessels of wild type mice but was absent in the respective samples from ALCAM<sup>-/-</sup> C57BL/6 mice (Figure 3(g)). Similarly,

ALCAM mRNA was detected in unstimulated and cytokine stimulated pMBMECs from wild type C57BL/6 mice (Figure 3(h)). Remarkably, the stimulation of pMBMECs with IL-1 $\beta$  induced a 3-fold upregulation of ALCAM mRNA, as compared to controls, whereas TNF- $\alpha$  caused no change (Figure 3(h)). At the same time, the levels of ICAM-1 or VCAM-1 mRNA were upregulated 23-fold and 8-fold upon stimulation pMBMECs with IL-1 $\beta$  (Figure 3(i) and (j)). Taken together, stimulation of pMBMECs with IL-1 $\beta$  induced a significant upregulation of ALCAM, ICAM-1, and VCAM-1.

### Endothelial ALCAM plays a limited role in mouse Th1 cell diapedesis across the BBB

We next investigated the role of ALCAM during diapedesis of Th1 cells in mouse. To specifically target the role of endothelial ALCAM, we took advantage of the ALCAM<sup>-/-</sup> C57BL/6 mouse as a source of pMBMECs.<sup>23,42</sup> ALCAM and CD6 protein expression on mouse encephalitogenic Th1 cells<sup>5,34</sup> was confirmed by flow cytometry (Supplementary Figure 5). Using the modified Boyden chamber assay, we found, in accordance with the observations made with human Th1 cells, a reduction of mouse Th1 cell diapedesis across unstimulated ALCAM<sup>-/-</sup> pMBMECs compared to wild type pMBMECs (Figure 4(a)). However, the difference was abrogated by the stimulation of pMBMECs with TNF- $\alpha$ , IL-1 $\beta$ , or TNF- $\alpha$ /IFN- $\gamma$  (Figure 4(a)). Compensatory upregulation of ICAM-1, ICAM-2, or VCAM-1 in the absence of ALCAM on stimulated ALCAM<sup>-/-</sup> compared to wild type pMBMECs was ruled out through side-by-side analysis of their cell surface expression (data not shown). Possibly, low levels of ALCAM on resting BBB-ECs contribute to Th1 cell migration, but ALCAM may become dispensable when other molecules involved in T cell extravasation, such as ICAM-1 or VCAM-1, are upregulated under inflammatory conditions.

To dissect the precise role of endothelial ALCAM leading to reduced Th1 cell diapedesis, we next employed *in vitro* time-lapse live cell imaging under physiological flow.<sup>38</sup> This approach has proven valuable for dissecting the different roles of other CAMs during the extravasation cascade across the BBB.<sup>5,6,43</sup> First, we compared the shear resistant arrest of Th1 cells on the unstimulated or cytokine stimulated wild type or ALCAM<sup>-/-</sup> pMBMECs (Figure 4(b)). Irrespective of the presence or absence of cytokine stimulation, we found comparable numbers of Th1 cells arresting on wild type and ALCAM<sup>-/-</sup> pMBMECs (Figure 4(b)), demonstrating that ALCAM does not contribute to mouse Th1 cell arrest on the BBB. Next, we compared the dynamic

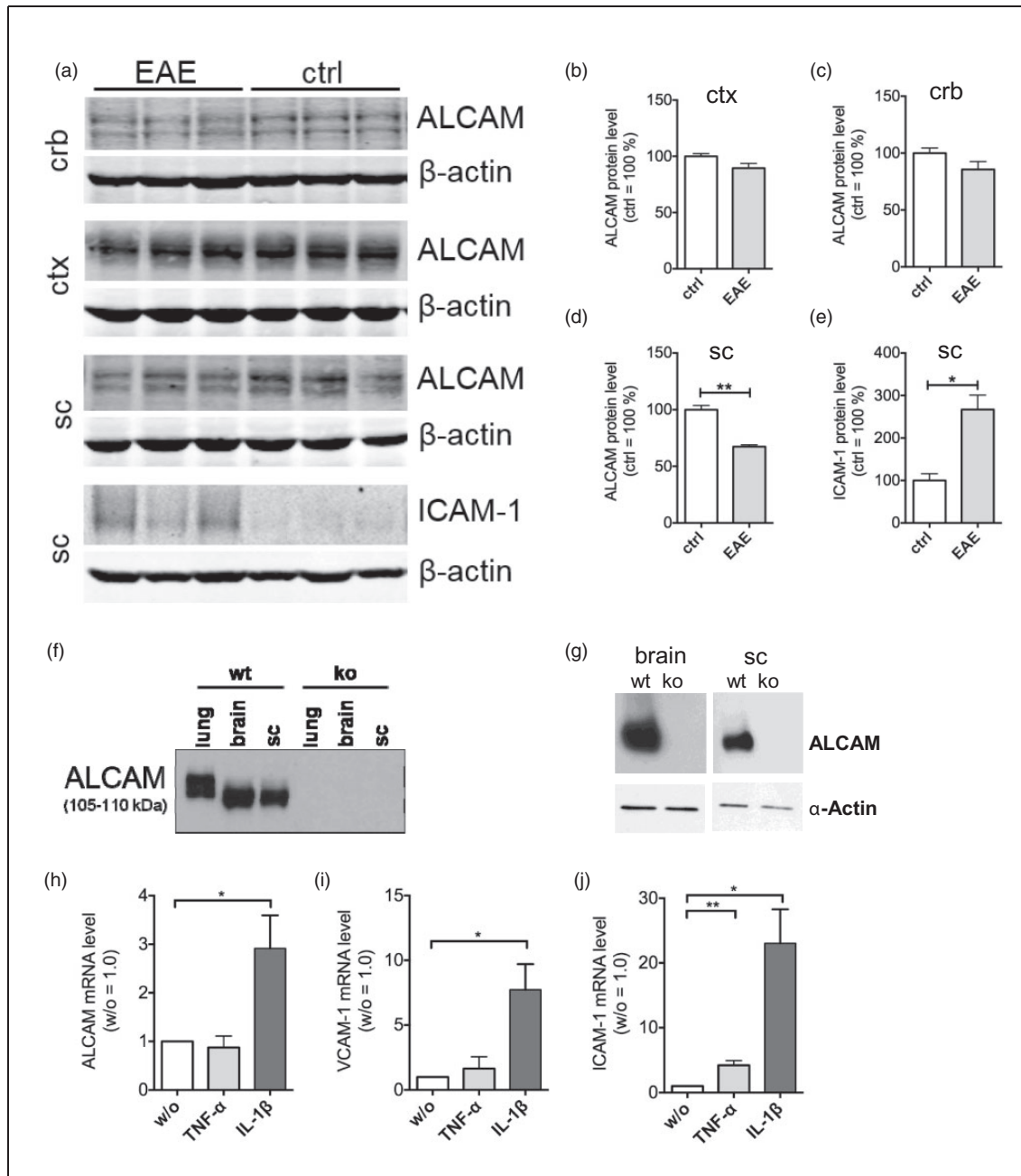


**Figure 3.** ALCAM expression in the mouse CNS and on the mouse BBB. (a) ALCAM or ICAM-1 protein in lysates from the brain cortex (ctx), cerebellum (crb), or spinal cord (sc) of wild type mice afflicted with acute paraplegic EAE or healthy gender and age matched control mice by Western Blot. Each lane represents protein samples from one individual mouse. Staining of  $\beta$ -actin proves equal loading, which was 20  $\mu$ g/lane. (b–e) Quantitative densitometry evaluation of the Western Blot shown in (a). ALCAM or ICAM-1 signal intensities were normalized to  $\beta$ -actin and expressed as fractions of the healthy control set to 100%. A detailed description of signal quantification is presented in Supplementary Figure 3 and Supplementary Table 2. (f) Analysis of ALCAM protein in whole tissue lysates of the lung, brain, or spinal cord (sc) from a wild type (wt) or an ALCAM<sup>-/-</sup> (ko) mouse by Western Blot. (g) ALCAM protein in brain (left) or spinal cord (right, sc) microvessel lysates from healthy wild type (wt) or ALCAM<sup>-/-</sup> (ko) mice was assessed by Western Blot. Equal loading (20  $\mu$ g/lane of brain vessels, 9  $\mu$ g/lane of spinal cord vessels) was ensured by  $\alpha$ -actin staining in parallel. (a, f, g) Detection of ALCAM was with the polyclonal anti mouse/human ALCAM antibody. (h–j) Relative quantification of ALCAM, ICAM-1, and VCAM-1 mRNA level in RNA lysates from wild type pMBMECs that were unstimulated (open bars) or stimulated for 4 h with TNF- $\alpha$  (grey bars) or IL-1 $\beta$  (dark grey bars) as assessed by qPCR. Unstimulated condition was set to 1.0. Bars show the mean  $\pm$  SD from five independent experiments, each performed in triplicate.

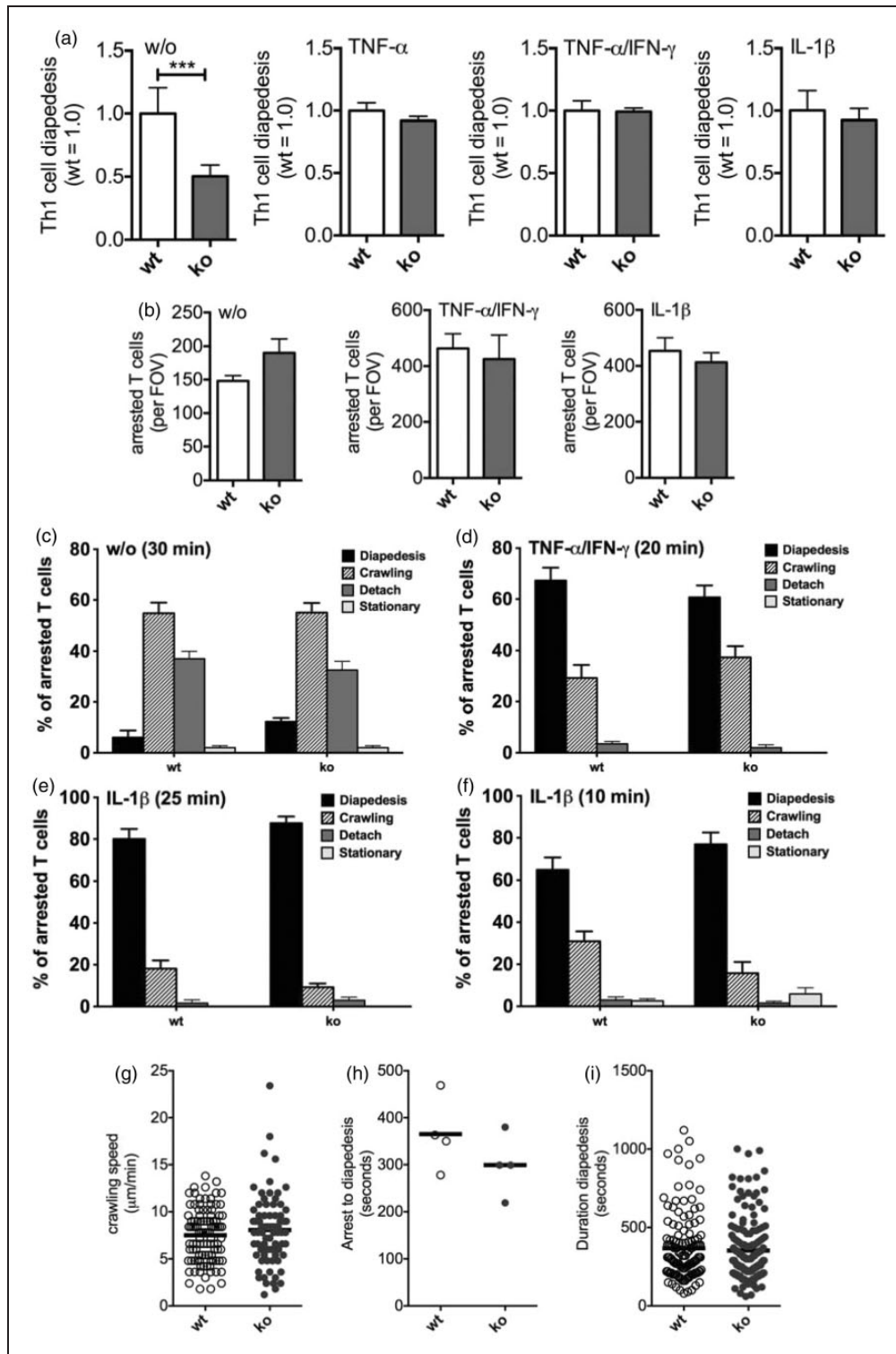


**Figure 4.** Comparison of mouse CD4<sup>+</sup> Th1 cell interaction with ALCAM<sup>-/-</sup> or wild type pMBMECs. (a) Diapedesis of CD4<sup>+</sup> Th1 cells across wild type (wt, white bars) or ALCAM<sup>-/-</sup> (ko, gray bars) pMBMECs was tested under static conditions. pMBMECs were without cytokine stimulation (w/o) or stimulated with TNF- $\alpha$ , TNF- $\alpha$ /IFN- $\gamma$ , or IL-1 $\beta$  as labeled. Diapedesis of mouse Th1 cells across ALCAM<sup>-/-</sup> (ko) is shown relative to Th1 cell diapedesis across wild type pMBMECs (wt) set to 1.0. Data are mean of 10 samples from three independent experiments (w/o) or mean of six samples (TNF- $\alpha$ , TNF- $\alpha$ /IFN- $\gamma$ ) or three samples (IL-1 $\beta$ ) from one representative experiment. Error bars are SD. (b-i) Dynamic interaction behavior of mouse Th1 cells on wild type (wt) or ALCAM<sup>-/-</sup> (ko) pMBMECs evaluated through in vitro live cell time lapse imaging under physiological flow. (b-f) pMBMECs were without cytokine stimulation

post-arrest behavior of Th1 cells on ALCAM<sup>-/-</sup> and wild type pMBMECs (Figure 4(c) to (i)). On unstimulated wild type pMBMECs, the majority of the arrested Th1 cells continuously crawled on the endothelial surface and another substantial fraction detached due to low sustained adhesive interactions, while only a minor fraction of the Th1 cells migrated across the pMBMEC monolayer (Figure 4(c)). In contrast, the majority of arrested Th1 cells crossed the cytokine stimulated-endothelial monolayer and another substantial fraction of Th1 cells continuously crawled on the endothelial surface with only rare events of detachment (Figure 4(d) and (e)). Importantly, the comparison of the dynamic Th1 cell behavior on wild type versus ALCAM<sup>-/-</sup> pMBMECs did not show any significant differences (Figure 4(c) to (e)). We also assessed shorter periods of evaluation to focus on early diapedesis which, however, did not reveal any significant difference in the dynamic Th1 cell behavior on wild type versus ALCAM<sup>-/-</sup> pMBMECs (Figure 4(e) and (f)). Furthermore, the speed of Th1 cell crawling (Figure 4(g)), the time elapsed between Th1 cell arrest and diapedesis (Figure 4(h)), or the duration of diapedesis (Figure 4(i)) were comparable on wild type and ALCAM<sup>-/-</sup> pMBMECs. Taken together, our detailed live cell imaging analysis did not reveal any role for endothelial ALCAM in the multi-step Th1 cell migration across mouse BBB-ECs in vitro. Thus, the observed role for endothelial ALCAM in mediating Th1 cell diapedesis across the BBB under static conditions is abrogated under physiological flow.

### *ALCAM is involved in multiple steps of monocyte migration across the BBB*

Considering our previous findings on ameliorated EAE upon anti-ALCAM treatment<sup>11</sup> but the limited role of ALCAM in Th1 cell diapedesis across the BBB, we finally aimed to delineate the role of ALCAM in monocyte migration across the BBB. After extravasation across the BBB, monocytes can differentiate into dendritic cells (DCs) and macrophages and contribute to disease pathogenesis.<sup>44,45</sup> Here, we used ex vivo sorted human CD14<sup>+</sup> monocytes of which 60 to 85%

expressed ALCAM, as demonstrated by us and others before.<sup>11,46</sup> Using the in vitro flow system, ex vivo human CD14<sup>+</sup> monocytes were allowed to interact with HBECs over a period of 30 min and were recorded in real time for multiple intervals of 30 sec. Tracking of individual monocytes over time demonstrated that blocking both, monocyte and endothelial ALCAM with a function-blocking antibody significantly reduced monocyte/HBEC interactions and interfered with an overall decrease in monocyte speed, as compared to the isotype control (Figure 5(a)). More specifically, anti-ALCAM antibody treatment blocked both, rolling (Figure 5(b)) and firm adhesion (Figure 5(c)) of CD14<sup>+</sup> monocytes on unstimulated HBECs. The function-blocking anti-ALCAM antibody also significantly reduced firm adhesion of CD14<sup>+</sup> monocytes on TNF- $\alpha$ /IFN- $\gamma$  stimulated HBECs (Figure 5(d)). Using the modified Boyden chamber assay, we found that antibody-mediated blocking of ALCAM reduced the migration of CD14<sup>+</sup> monocytes across resting HBECs (Figure 5(e)). We also correlated the diapedesis of monocytes across HMECs obtained from the same donors as the HBECs. As expected, monocytes migrated in higher numbers across the more permeable HMECs, while also being significantly blocked upon the addition of anti-ALCAM antibodies (Figure 5(e)). Importantly, the effect of antibody-mediated inhibition of ALCAM on monocyte diapedesis was comparable to the extent of antibody-mediated blockage of ICAM-1 (Figure 5(e)). In conclusion, ALCAM contributes to the extravasation of human CD14<sup>+</sup> monocytes across the human BBB at various individual steps, namely rolling, firm adhesion, and diapedesis. Thus, we conclude that a therapeutic targeting of ALCAM in the treatment of neuroinflammation would affect the recruitment of monocytes into the CNS but exert limited effect on the recruitment of CD4<sup>+</sup> effector T cells.

## Discussion

MS is an inflammatory disease of the CNS with no cure available to date. However, treatments exist that ameliorate and delay the progression of the disease. Successful therapeutic strategies targeting immune cell

### **Figure 4.** Continued

(w/o) or stimulated with IL-1 $\beta$  or TNF- $\alpha$ /IFN- $\gamma$  as indicated. Values are the mean of three independent experiments. (b) Numbers of arrested Th1 cells per field of view (FOV). (c–f) Dynamic post-arrest interaction of the Th1 cells on the pMBMECs is described in four behavioral categories: Diapedesis (black bars), crawling but no diapedesis (hatched bars), detachment (dark gray bars), or stationary (light gray bars). Numbers of arrested Th1 cells were set to 100% and the behavioral categories are expressed in fractions of arrested T cells. Period of observation was 30 min ((c), w/o), 20 min ((d), TNF- $\alpha$ /IFN- $\gamma$ ) or 25 and 10 min ((e, f), IL-1 $\beta$ ). (g) Crawling speed of Th1 cells on the surface of IL-1 $\beta$  stimulated pMBMECs. Each dot represents the crawling speed of one Th1 cell. (h) Time elapsed between initial arrest and start of diapedesis in seconds on IL-1 $\beta$  stimulated pMBMECs. Each dot represents mean values from at least 50 CD4<sup>+</sup> Th1 cells in one experiment. (i), duration of T cell diapedesis across IL-1 $\beta$  stimulated pMBMECs. Each dot represents one T cell.

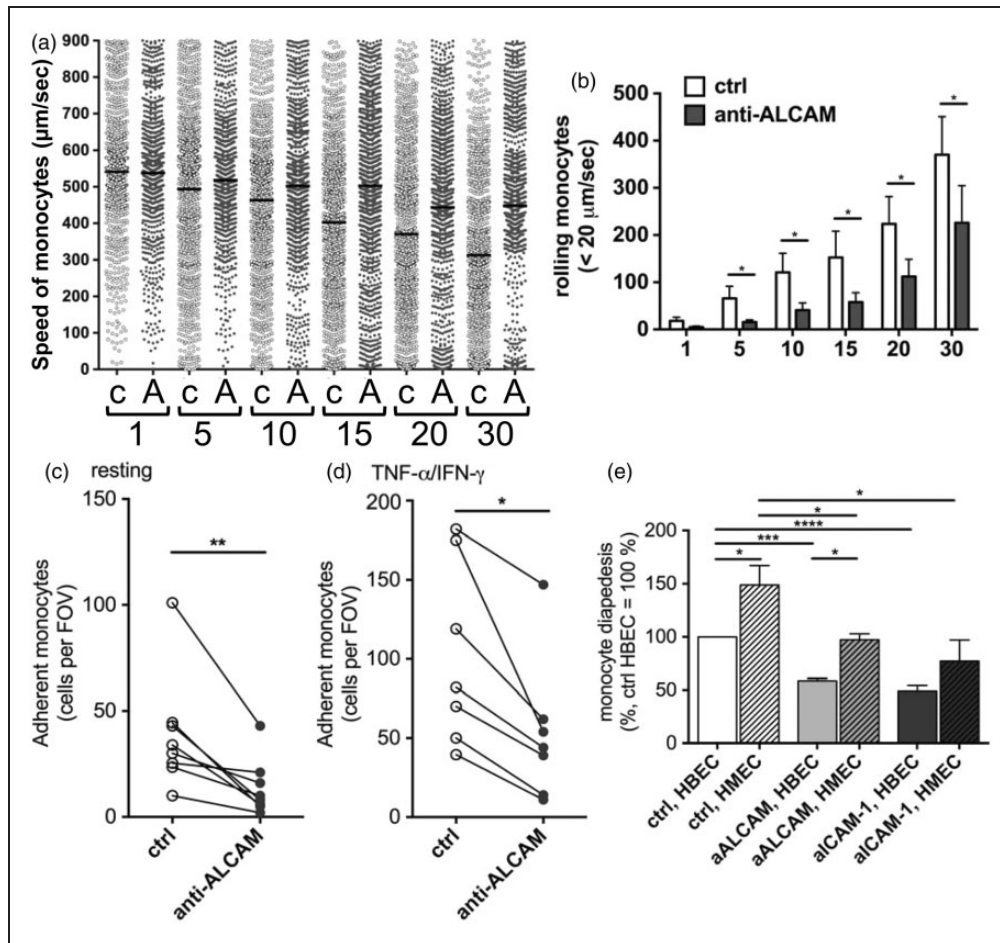


**Figure 5.** Role of ALCAM in the extravasation of human monocytes across the human BBB. (a–d) Monocyte/HBEC interactions were analyzed under flow conditions. HBECs and CFSE-labeled human CD14<sup>+</sup> monocytes were treated with a function-blocking anti-ALCAM antibody or isotype control ( $n = 7$  individual experiments). (a) Monocytes were perfused over HBECs and 30-sec-movies were acquired at 1 min, 5 min, 10 min, 15 min, 20 min, or 30 min (x-axis: 1, 5, 10, 15, 20, 30; c, ctrl; A, anti-ALCAM). Each dot represents the mean velocity of a single CFSE<sup>+</sup> cell. The horizontal bars are representative of the mean per data set. (b) Numbers of rolling monocytes (1–20 µm/sec) per FOV at 1 min, 5 min, 10 min, 15 min, 20 min, or 30 min after monocyte perfusion are shown. (c–d) Numbers of adherent CD14<sup>+</sup> monocytes on resting (c) or cytokine (TNF-α/IFN-γ) (d) stimulated HBECs 20 min after monocyte perfusion. Monocytes from individual healthy donors are compared side-by-side (horizontal lines). (e) Diapedesis of human monocytes across HBECs or HMECs; both cell types were pre-treated with ALCAM or ICAM-1 blocking antibodies or isotype control antibody ( $n = 4$ ). HBECs and HMECs from identical donors were tested side-by-side and diapedesis rates were normalized to monocyte diapedesis across isotype control treated HBECs (100%). Antibodies were anti ALCAM clone 105,901 (a–e) and anti ICAM-1 clone BBA3 (e).

trafficking have been translated into the clinics such as the humanized anti-α4-integrin antibody natalizumab and the sphingosine-analogue fingolimod.<sup>2,3</sup> Unfortunately, natalizumab and fingolimod harbor a low risk of developing the fatal disease PML, which is due to the complete inhibition of the CNS immune surveillance.<sup>47,48</sup> To define alternative therapeutic targets aimed at inhibiting pathological immune cell entry into the CNS during MS, more detailed knowledge on the multi-step extravasation of different immune cell subsets across the BBB is required. In previous studies, we have defined the individual roles of endothelial selectins, VCAM-1, ICAM-1, and ICAM-2 in

CD4<sup>+</sup> Th1 cell extravasation across the BBB during EAE.<sup>5,6,49,50</sup> However, further endothelial cell surface proteins expressed at the BBB, such as melanoma cell adhesion molecule (MCAM, CD146),<sup>30,51</sup> netrin-1,<sup>29</sup> Ninjurin-1,<sup>39,52</sup> and ALCAM<sup>11</sup> were recently proposed as additional players in the migration of different immune cell subsets including Th1 and Th17 cells across the BBB and hence as potential pharmaceutical targets for the treatment of MS. However, the precise steps mediated by these additional molecules within the extravasation cascade have not been solved. To this end, we here analyzed the role of ALCAM in various

---

steps of extravasation using human Th1 or Th17 cells and monocytes, as well as mouse Th1 cells across both human and mouse *in vitro* models of the BBB. Functional analysis was complemented by the analysis of ALCAM expression in human and mouse CNS tissue or on their respective *in vitro* models of the BBB.

In a previous study, we found increased ALCAM expression on brain vessels in acute MS lesions.<sup>11</sup> Similarly, inflamed vessels in the CNS of drug-abusing or HIV-infected patients<sup>53</sup> show increased ALCAM expression. In the present study, we confirmed the expression of ALCAM protein in human brain BBB-ECs. However, we also found that, in chronic MS lesions, vascular ALCAM is not enhanced compared to NAWM or control tissues from individuals without neurological diseases. Obviously, specific inflammatory conditions play a decisive role in the upregulation of ALCAM at the human BBB *in situ*. On the other hand, ALCAM was readily detectable on both, unstimulated stem cell- and primary cell-derived *in vitro* models of the human BBB and increased upon cytokine stimulation in line with our previous observations.<sup>11</sup> Thus, our data confirm the expression of ALCAM on the human BBB *in situ* and *in vitro*.

In our previous study, we have demonstrated a role for ALCAM in the diapedesis of human CD4<sup>+</sup> but not CD8<sup>+</sup> T cells across the human BBB.<sup>11</sup> In apparent contrast, another study failed to find a role for endothelial ALCAM in the migration of human CD3<sup>+</sup> T cells across an *in vitro* model of the human BBB consisting of commercially available human brain microvascular ECs co-cultured with astrocytes.<sup>46</sup> However, the latter study was based on a different experimental setup including a chemotaxis component towards CCL2 or CXCL12, longer duration of the T cell migration period and a different anti-ALCAM antibody.<sup>46</sup> In addition, the more heterogeneous population of CD3<sup>+</sup> T cells investigated in that study might have superseded the role of ALCAM in mediating the diapedesis of specific T cell subsets across the BBB. The role of ALCAM in the extravasation of CD4<sup>+</sup> Th1 and Th17 cells has not been addressed hitherto. Here, we confirmed the role of ALCAM in the diapedesis of mixed populations of *ex vivo* CD4<sup>+</sup> T cells across unstimulated HBECs. However, antibody-mediated inhibition of ALCAM neither blocked rolling nor flow resistant arrest of *in vitro* polarized human Th1 cells nor adhesion of *ex vivo* sorted human Th1 cells to unstimulated or stimulated HBECs or HBLECs, respectively. Nonetheless, antibody-mediated inhibition of ALCAM significantly reduced the diapedesis of *in vitro* polarized human Th1 cells across HBECs but neither adhesion nor diapedesis of human Th17 cells. Thus, our results suggest that ALCAM

plays a limited role in T cell extravasation across the BBB by contributing solely to the diapedesis of human CD4<sup>+</sup> Th1 but not Th17 cells across the human BBB.

Research based on mouse species offering knock-out models for *in vivo* and *in vitro* studies for the inhibition of leukocyte trafficking has been fundamental for the clinic.<sup>3,41</sup> To set the stage, we here investigated the expression of ALCAM in the mouse CNS and its role in Th1 cell extravasation across the BBB. We determined that either equal or lower amount of ALCAM protein is present in the brain or spinal cord of C57BL/6 mice during acute EAE. The inflamed condition of the samples was confirmed by the upregulation of ICAM-1 compared to control samples.<sup>54,55</sup> While the expression of ALCAM on neurons has been described before,<sup>23,56</sup> we here confirmed ALCAM expression *in situ* on neurons and in the meningeal layers, whereas the parenchymal CNS vasculature did not visibly stain positive for ALCAM. We concluded that in contrast to the human brain, ALCAM protein in mouse CNS vessels might be difficult to detect due to its low level compared to its high level in neurons.

To test whether the role of ALCAM in the diapedesis of Th1 cells across the BBB is conserved between human and mouse in spite of the obvious differences in ALCAM protein levels on the BBB, we used encephalitogenic mouse Th1 cells<sup>42</sup> and a mouse *in vitro* BBB model composed of pMBMECs.<sup>28,37</sup> Isolation of pMBMECs from ALCAM<sup>-/-</sup> C57BL/6 mice<sup>21</sup> and wild type littermates in parallel enabled a direct comparison of Th1 cell interaction with the BBB in the presence or absence of ALCAM. To model an inflamed BBB with high levels of ICAM-1 and VCAM-1, pMBMECs were stimulated with pro-inflammatory cytokines.<sup>5,6</sup> Under static conditions, mouse Th1 cell diapedesis was reduced across unstimulated ALCAM<sup>-/-</sup> compared to wild type pMBMECs. *In vitro* live cell imaging under physiological flow has proven valuable in delineating the different roles of endothelial ICAM-1, ICAM-2, and VCAM-1 during the extravasation of immune cell subsets across the BBB.<sup>5,6,37,57,58</sup> Interestingly, our detailed analysis revealed comparable Th1 cell shear resistant arrest, diapedesis, crawling speed, or duration of diapedesis on wild type and ALCAM<sup>-/-</sup> pMBMECs. Upon stimulation with pro-inflammatory cytokines, the diapedesis rate of mouse Th1 cells across ALCAM<sup>-/-</sup> or wild type pMBMECs was also equal under static and under flow conditions. Following the strong upregulation of mouse endothelial ICAM-1 and VCAM-1 upon cytokine stimulation as compared to ALCAM and considering their essential roles in the multi-step extravasation cascade, our data suggest that ALCAM could be involved in the diapedesis of mouse Th1 cells across the BBB in unstimulated low shear stress

conditions in vivo, but becomes dispensable during neuroinflammation.<sup>5,6</sup>

To explain the prominent role of ALCAM previously observed during the development of EAE,<sup>11</sup> we investigated the role of monocytes, which can differentiate into DCs and macrophages after infiltrating the CNS and thus contribute to EAE and MS pathogenesis.<sup>59</sup> In particular, early depletion of monocytes completely abrogates clinical development of EAE<sup>45</sup> and depletion of monocytes after disease onset still protects from axonal loss during EAE.<sup>60</sup> This led us to finally analyze the role of ALCAM in various steps of monocyte extravasation across the BBB. We here confirmed a significant role of ALCAM in monocyte diapedesis across unstimulated and cytokine stimulated HBECs that previous studies have described before.<sup>11,46,61</sup> In the present study, we found additional roles for ALCAM during monocyte rolling and shear resistant arrest on the human BBB not addressed by others hitherto. Possibly, higher levels of ALCAM on monocytes versus Th1 or Th17 cells could explain the increased effect of blocking ALCAM on the multi-step extravasation of monocytes across the BBB, as compared to the T cell subsets. In support, overexpression of ALCAM on the surface of human T-lymphotropic virus type 1 (HTLV-1)-infected lymphocytes was identified as a cause for their increased migration across the human BBB.<sup>62</sup>

In conclusion, we here demonstrate a higher expression of ALCAM on the human BBB, as compared to the mouse BBB. Nevertheless, in both species, ALCAM is involved in the diapedesis of Th1 cells across the uninfamed BBB, though it is not involved in shear resistant arrest, adhesion strengthening, and diapedesis of Th1 cells under flow. In contrast, the prominent role of ALCAM in multiple steps of the monocyte extravasation cascade across the BBB suggests that the function-blocking anti-ALCAM antibody specifically interferes with monocyte infiltration into the CNS during autoimmune neuroinflammation and thus lead to the amelioration of EAE as observed before.<sup>11</sup> Considering the prominent expression of ALCAM on the human BBB, ALCAM might be a suitable therapeutic target for specifically targeting myeloid cell migration into the CNS, while leaving T cell-mediated CNS immune surveillance intact.

### Funding

The author(s) disclosed receipt of the following financial support for the research, authorship, and/or publication of this article: This work was financially supported by grants from the Swiss Multiple Sclerosis Society to RL and to NSW and by grants from the Multiple Sclerosis Society of Canada (MSSOC) and ERA-NET NEURON MELTRA BBB consortium (European Commission and CIHR/FRQS) to AP.

Further funding was from the Swiss National Science Foundation (SNSF), grant no. 31003A 133092 to RL and BE, and 31003A 141185 to NSW, the SNSF funded ProDoc Program “Cell Migration” grants no. PDFMP3 137079 and PDAMP3 137087 to BE and RL, the Swiss University Conference, Sinergia UnmetMS CRSII3\_154483 to BE and FS, the Germanine de Stael program to FG and BE and the Microscopy Imaging Center of the University of Bern. MAL holds a scholarship from Fonds de Recherche du Québec-Santé (FRQS). LM holds a scholarship from the MSSOC. AP holds a Senior Scholar Award of the FRQS and holds a senior Canada Research Chair in Multiple Sclerosis. MA and AG were enrolled in the Graduate School for Biomedical and Cellular Sciences of the University of Bern.

### Acknowledgements

We thank Dr. Cornelia Halin (ETH Zürich, Switzerland) for providing the ALCAM<sup>-/-</sup> C57BL/6 mice. Mark Liebi, Therese Périnat, Claudia Blatti, Lyne Bourbonnière, and Sandra Larouche receive our thanks for expert technical assistance. Special thanks go to Dr. Silvia Tietz for providing protein samples.

### Declaration of conflicting interests

The author(s) declared no potential conflicts of interest with respect to the research, authorship, and/or publication of this article.

### Authors' contributions

AG, CW, CM, FG, JW, LM, MA, MR, LM, and TZ each made substantial contributions to performing experiments, acquisition, and analysis of data. FS, GE, NSW, and UD contributed to design of the study and provided input to the manuscript. MAL and RL substantially contributed with concept and design of the experiments, writing of the manuscript and acquisition, analysis and interpretation of data. AP and BE were involved in the overall design of the study and made substantial contributions to writing the manuscript.

### Supplementary material

Supplementary material for this paper can be found at <http://jcbfm.sagepub.com/content/by/supplemental-data>

### References

1. Keaney J and Campbell M. The dynamic blood-brain barrier. *FEBS J* 2015; 282: 4067–4079.
2. Lopes Pinheiro MA, Kooij G, Mizze MR, et al. Immune cell trafficking across the barriers of the central nervous system in multiple sclerosis and stroke. *Biochim Biophys Acta* 2016; 1862: 461–471.
3. Engelhardt B and Kappos L. Natalizumab: targeting alpha4-integrins in multiple sclerosis. *Neurodegen Dis* 2008; 5: 16–22.
4. Lyck R and Engelhardt B. Going against the tide – how encephalitogenic T cells breach the blood-brain barrier. *J Vasc Res* 2012; 49: 497–509.

5. Steiner O, Coisne C, Cecchelli R, et al. Differential roles for endothelial ICAM-1, ICAM-2, and VCAM-1 in shear-resistant T cell arrest, polarization, and directed crawling on blood-brain barrier endothelium. *J Immunol* 2010; 185: 4846–4855.
6. Abadier M, Haghayegh JN, Cardoso AL, et al. Cell surface levels of endothelial ICAM-1 influence the transcellular or paracellular T-cell diapedesis across the blood-brain barrier. *Eur J Immunol* 2015; 45: 1043–1058.
7. Bartholomaeus I, Kawakami N, Odoardi F, et al. Effector T cell interactions with meningeal vascular structures in nascent autoimmune CNS lesions. *Nature* 2009; 462: 94–98.
8. Sage PT and Carman CV. Settings and mechanisms for trans-cellular diapedesis. *Front Biosci* 2009; 14: 5066–5083.
9. Carman CV. Mechanisms for transcellular diapedesis: probing and pathfinding by ‘invadosome-like protrusions’. *J Cell Sci* 2009; 122: 3025–3035.
10. Kawakami N and Flugel A. Knocking at the brain’s door: intravital two-photon imaging of autoreactive T cell interactions with CNS structures. *Sem Immunopathol* 2010; 32: 275–287.
11. Cayrol R, Wosik K, Berard JL, et al. Activated leukocyte cell adhesion molecule promotes leukocyte trafficking into the central nervous system. *Nat Immunol* 2008; 9: 137–145.
12. Bowen MA, Patel DD, Li X, et al. Cloning, mapping, and characterization of activated leukocyte-cell adhesion molecule (ALCAM), a CD6 ligand. *J Exp Med* 1995; 181: 2213–2220.
13. Pourquie O, Corbel C, Le Caer JP, et al. BEN, a surface glycoprotein of the immunoglobulin superfamily, is expressed in a variety of developing systems. *Proc Natl Acad Sci U S A* 1992; 89: 5261–5265.
14. Matsumoto A, Mitchell A, Kurata H, et al. Cloning and characterization of HB2, a candidate high density lipoprotein receptor. Sequence homology with members of the immunoglobulin superfamily of membrane proteins. *J Biol Chem* 1997; 272: 16778–16782.
15. van Kempen LC, Nelissen JM, Degen WG, et al. Molecular basis for the homophilic activated leukocyte cell adhesion molecule (ALCAM)-ALCAM interaction. *J Biol Chem* 2001; 276: 25783–25790.
16. Bowen MA and Aruffo A. Adhesion molecules, their receptors, and their regulation: analysis of CD6-activated leukocyte cell adhesion molecule (ALCAM/CD166) interactions. *Transplant Proc* 1999; 31: 795–796.
17. Gangemi RM, Swack JA, Gaviria DM, et al. Anti-T12, an anti-CD6 monoclonal antibody, can activate human T lymphocytes. *J Immunol* 1989; 143: 2439–2447.
18. Morimoto C, Rudd CE, Letvin NL, et al. 2H1 – a novel antigen involved in T lymphocyte triggering. *J Immunol* 1988; 140: 2165–2170.
19. Hassan NJ, Barclay AN and Brown MH. Frontline: optimal T cell activation requires the engagement of CD6 and CD166. *Eur J Immunol* 2004; 34: 930–940.
20. Wagner M, Wisniewski A, Bilinska M, et al. ALCAM – novel multiple sclerosis locus interfering with HLA-DRB1\*1501. *J Neuroimmunol* 2013; 258: 71–76.
21. Kofler DM, Severson CA, Mousissian N, et al. The CD6 multiple sclerosis susceptibility allele is associated with alterations in CD4+ T cell proliferation. *J Immunol* 2011; 187: 3286–3291.
22. De Jager PL, Jia X, Wang J, et al. Meta-analysis of genome scans and replication identify CD6, IRF8 and TNFRSF1A as new multiple sclerosis susceptibility loci. *Nat Genet* 2009; 41: 776–782.
23. Weiner JA, Koo SJ, Nicolas S, et al. Axon fasciculation defects and retinal dysplasias in mice lacking the immunoglobulin superfamily adhesion molecule BEN/ALCAM/SC1. *Mol Cell Neurosci*. 2004; 27: 59–69.
24. Pedroso DC, Tellechea A, Moura L, et al. Improved survival, vascular differentiation and wound healing potential of stem cells co-cultured with endothelial cells. *PLoS One* 2011; 6: e16114.
25. Cecchelli R, Aday S, Sevin E, et al. A stable and reproducible human blood-brain barrier model derived from hematopoietic stem cells. *PLoS One* 2014; 9: e99733.
26. Prat A, Biernacki K, Becher B, et al. B7 expression and antigen presentation by human brain endothelial cells: requirement for proinflammatory cytokines. *J Neuropathol Exp Neurol* 2000; 59: 129–136.
27. Ifergan I, Wosik K, Cayrol R, et al. Statins reduce human blood-brain barrier permeability and restrict leukocyte migration: relevance to multiple sclerosis. *Ann Neurol* 2006; 60: 45–55.
28. Lyck R, Ruderisch N, Moll AG, et al. Culture-induced changes in blood-brain barrier transcriptome: implications for amino-acid transporters in vivo. *J Cereb Blood Flow Metab* 2009; 29: 1491–1502.
29. Podjaski C, Alvarez JI, Bourbonniere L, et al. Netrin 1 regulates blood-brain barrier function and neuroinflammation. *Brain* 2015; 138: 1598–1612.
30. Larochele C, Lecuyer MA, Alvarez JI, et al. Melanoma cell adhesion molecule-positive CD8 T lymphocytes mediate central nervous system inflammation. *Ann Neurol* 2015; 78: 39–53.
31. Kebir H, Kreyenborg K, Ifergan I, et al. Human TH17 lymphocytes promote blood-brain barrier disruption and central nervous system inflammation. *Nat Med* 2007; 13: 1173–1175.
32. Engen SA, Valen Rukke H, Becattini S, et al. The oral commensal *Streptococcus mitis* shows a mixed memory Th cell signature that is similar to and cross-reactive with *Streptococcus pneumoniae*. *PLoS One* 2014; 9: e104306.
33. Sallusto F, Schaerli P, Loetscher P, et al. Rapid and coordinated switch in chemokine receptor expression during dendritic cell maturation. *Eur J Immunol* 1998; 28: 2760–2769.
34. Laschinger M and Engelhardt B. Interaction of alpha4-integrin with VCAM-1 is involved in adhesion of encephalitogenic T cell blasts to brain endothelium but not in their transendothelial migration in vitro. *J Neuroimmunol* 2000; 102: 32–43.
35. Weil MT, Mobius W, Winkler A, et al. Loss of myelin basic protein function triggers myelin breakdown in models of demyelinating diseases. *Cell Rep* 2016; 16: 314–322.

- 
36. Alvarez JI, Dodelet-Devillers A, Kebir H, et al. The Hedgehog pathway promotes blood-brain barrier integrity and CNS immune quiescence. *Science* 2011; 334: 1727–1731.
  37. Steiner O, Coisne C, Engelhardt B, et al. Comparison of immortalized bEnd5 and primary mouse brain microvascular endothelial cells as in vitro blood-brain barrier models for the study of T cell extravasation. *J Cereb Blood Flow Metab* 2011; 31: 315–327.
  38. Coisne C, Lyck R and Engelhardt B. Live cell imaging techniques to study T cell trafficking across the blood-brain barrier in vitro and in vivo. *Fluids Barriers CNS* 2013; 10: 7.
  39. Ifergan I, Kebir H, Terouz S, et al. Role of Ninjurin-1 in the migration of myeloid cells to central nervous system inflammatory lesions. *Ann Neurol* 2011; 70: 751–763.
  40. Sallusto F, Lenig D, Mackay CR, et al. Flexible programs of chemokine receptor expression on human polarized T helper 1 and 2 lymphocytes. *J Exp Med* 1998; 187: 875–883.
  41. Krishnamoorthy G and Wekerle H. EAE: an immunologist's magic eye. *Eur J Immunol* 2009; 39: 2031–2035.
  42. Engelhardt B, Laschinger M, Schulz M, et al. The development of experimental autoimmune encephalomyelitis in the mouse requires alpha4-integrin but not alpha4-beta7-integrin. *J Clin Invest* 1998; 102: 2096–2105.
  43. Bartholomaeus I, Kawakami N, Odoardi F, et al. Effector T cell interactions with meningeal vascular structures in nascent autoimmune CNS lesions. *Nature* 2009; 462: 94–98.
  44. Mildner A, Mack M, Schmidt H, et al. CCR2+Ly-6Chi monocytes are crucial for the effector phase of autoimmunity in the central nervous system. *Brain* 2009; 132: 2487–2500.
  45. Fife BT, Huffnagle GB, Kuziel WA, et al. CC chemokine receptor 2 is critical for induction of experimental autoimmune encephalomyelitis. *J Exp Med* 2000; 192: 899–905.
  46. Williams DW, Anastos K, Morgello S, et al. JAM-A and ALCAM are therapeutic targets to inhibit diapedesis across the BBB of CD14+CD16+ monocytes in HIV-infected individuals. *J Leukoc Biol* 2015; 97: 401–412.
  47. Derfuss T, Kuhle J, Lindberg R, et al. Natalizumab therapy for multiple sclerosis. *Semin Neurol* 2013; 33: 26–36.
  48. Kappos L, Cohen J, Collins W, et al. Fingolimod in relapsing multiple sclerosis: an integrated analysis of safety findings. *Mult Scler Relat Disord* 2014; 3: 494–504.
  49. Sathyanadan K, Coisne C, Enzmann G, et al. PSGL-1 and E/P-selectins are essential for T-cell rolling in inflamed CNS microvessels but dispensable for initiation of EAE. *Eur J Immunol* 2014; 44: 2287–2294.
  50. Coisne C, Mao W and Engelhardt B. Cutting edge: natalizumab blocks adhesion but not initial contact of human T cells to the blood-brain barrier in vivo in an animal model of multiple sclerosis. *J Immunol* 2009; 182: 5909–5913.
  51. Duan H, Xing S, Luo Y, et al. Targeting endothelial CD146 attenuates neuroinflammation by limiting lymphocyte extravasation to the CNS. *Sci Rep* 2013; 3: 1687.
  52. Ahn BJ, Le H, Shin MW, et al. Ninjurin1 deficiency attenuates susceptibility of experimental autoimmune encephalomyelitis in mice. *J Biol Chem* 2014; 289: 3328–3338.
  53. Yao H, Kim K, Duan M, et al. Cocaine hijacks sigma1 receptor to initiate induction of activated leukocyte cell adhesion molecule: implication for increased monocyte adhesion and migration in the CNS. *J Neurosci* 2011; 31: 5942–5955.
  54. Wolburg K, Gerhardt H, Schulz M, et al. Ultrastructural localization of adhesion molecules in the healthy and inflamed choroid plexus of the mouse. *Cell Tissue Res* 1999; 296: 259–269.
  55. Bullard DC, Hu X, Schoeb TR, et al. Intercellular adhesion molecule-1 expression is required on multiple cell types for the development of experimental autoimmune encephalomyelitis. *J Immunol* 2007; 178: 851–857.
  56. Buhusi M, Demyanenko GP, Jannie KM, et al. ALCAM regulates mediolateral retinotopic mapping in the superior colliculus. *J Neurosci* 2009; 29: 15630–15641.
  57. Rudolph H, Klopstein A, Gruber I, et al. Post-arrest stalling rather than crawling favors CD8+ over CD4+ T-cell migration across the blood-brain barrier under flow in vitro. *Eur J Immunol* 2016; 46: 2187–2203.
  58. Gorina R, Lyck R, Vestweber D, et al. Beta2 integrin-mediated crawling on endothelial ICAM-1 and ICAM-2 is a prerequisite for transcellular neutrophil diapedesis across the inflamed blood-brain barrier. *J Immunol* 2014; 192: 324–337.
  59. Lussi F, Zipp F and Witsch E. Dendritic cells as therapeutic targets in neuroinflammation. *Cell Mol Life Sci* 2016; 73: 2425–2450.
  60. Moreno MA, Burns T, Yao P, et al. Therapeutic depletion of monocyte-derived cells protects from long-term axonal loss in experimental autoimmune encephalomyelitis. *J Neuroimmunol* 2016; 290: 36–46.
  61. Williams DW, Calderon TM, Lopez L, et al. Mechanisms of HIV entry into the CNS: increased sensitivity of HIV-infected CD14+CD16+ monocytes to CCL2 and key roles of CCR2, JAM-A, and ALCAM in diapedesis. *PLoS One* 2013; 8: e69270.
  62. Curis C, Percher F, Jeannin P, et al. Human T-lymphotropic virus (HTLV)-1-induced overexpression of activated leukocyte cell adhesion molecule (ALCAM) facilitates trafficking of infected lymphocytes through the blood-brain barrier. *J Virol* 2016; 90: 7303–7312.